Electronic Supporting Information (ESI)

Synthesis of Au nanorods−embedded and graphene oxide−wrapped microporous ZIF−8 with high electrocatalytic activity for the sensing of pesticides

Tian Gan,*[a,b] Jiebin Li,[a] Hanxiao Li,[a] Yangxiao Liu[a] and Zhihong Xu[b]

[a] *College of Chemistry and Chemical Engineering, Institute for Conservation and Utilization of Agro−Bioresources in Dabie Mountains & Henan Key Laboratory of Utilization of Non−Metallic Mineral in the South of Henan, Xinyang Normal University, Xinyang 464000, China. E-mail: gantianxynu@163.com*

[b] *Key Laboratory of Biomarker Based Rapid−Detection Technology for Food Safety of Henan Province, Food and Biological Engineering College, Xuchang University, Xuchang 461000, China*

XPS depth profile analysis of AuNRs@ZIF−8@GO

The AuNRs@ZIF−8@GO thin film was deposited by spin−coating (spin rate = 1500 rpm) on thoroughly cleaned ITO glass substrate (1 cm^2) for 30 s using a KW−4A spin coater (Institute of Microelectronics, Chinese Academy of Sciences), then dried at 60 °C in a vacuum oven for 1 h and this process was repeated ten times. The chemical composition of the AuNRs@ZIF−8@GO was done on a Thermo Scientific K−Alpha XPS spectrometer using a standard X−ray source of 15 kV, 300 W, and Al K_α (1484.8 eV). For sputter depth profiling, Ar^+ ions of 3 keV energy at a scan size of 2.4 × 2.4 mm was used. The absolute binding energies were referenced to the C 1s photoelectron peak at 284.8 eV originating from adventitious hydrocarbons in unsputtered surfaces.

Fig. S1 shows the XPS depth profile of the AuNRs@ZIF−8@GO film after a 4 min sputter time. Obviously, only Zn, O, N, C, and Au are obtained in the general survey spectrum (Fig. S1A), confirming the high purity of as−synthesized sample. Typical high resolution scan of Au 4f−Zn 3p displays a shoulder at the low binding energy side (Fig. S1B), which was deconvoluted using a standard software via symmetric Gaussian curves and a Shirly type background correction. Four separate peaks including Au $4f_{7/2}$ (83.4 eV), Au $4f_{5/2}$ (87.3 eV), Zn $3p_{3/2}$ (88.7 eV), and Zn $3p_{1/2}$ (91.5 eV) were resolved. It is evident that the interaction between Au and ZIF−8 would not influence the metallic property of the AuNRs which still existed at metallic state (Au^0). The high resolution spectrum of Zn 2p exhibits the occurrence of two intense peaks at binding energies of 1021.6 and 1044.6 eV resulting from Zn $2p_{3/2}$ and Zn $2p_{1/2}$, respectively (Fig. Fig. S1C). The spin−orbit splitting is observed to be 23 eV, close to that of Zn^{2+} (ΔE = 22.97 eV).[1] From the C1s spectrum in Fig. S1D, a strong

peak centered at 284.5 eV (C−C/C=C) is dominant. In addition, the binding energy peaks located at 285.5 and 286.9 eV relating to the carbon atoms in C−N bond of ZIF−8 and carbonyl (C=O) of GO can be seen. It is noteworthy that the absence of other oxygen−containing functional groups (i.e. epoxy, hydroxyl, and carboxylic) illustrates the chemical interaction between ZIF−8 and GO.[2,3]

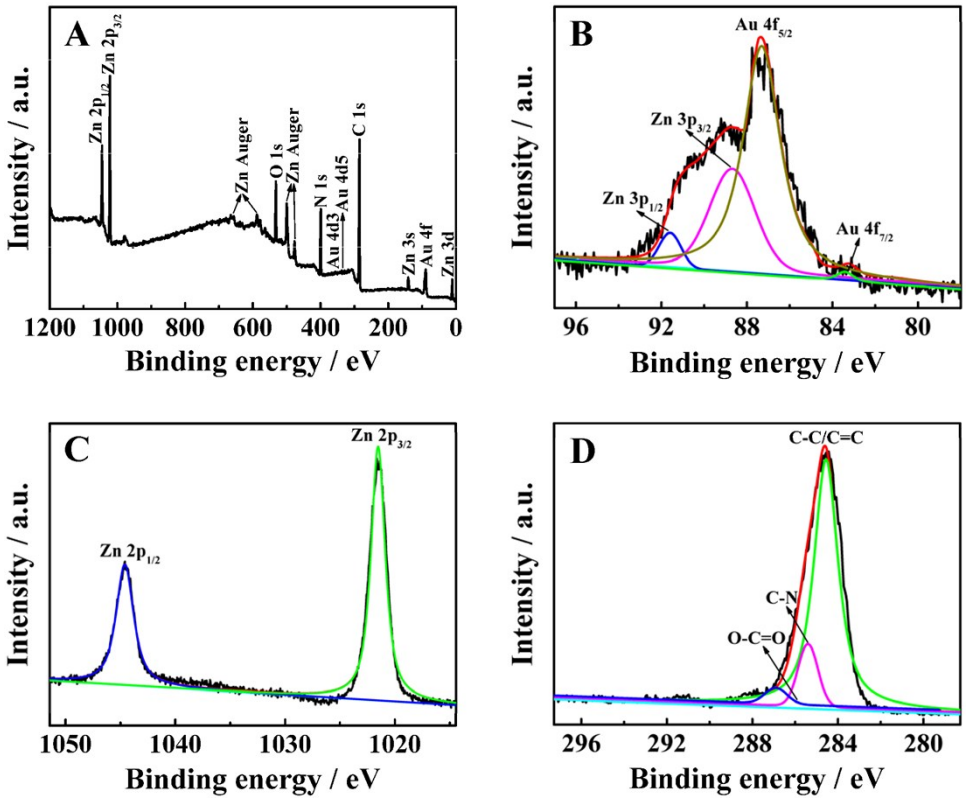

Fig. S1 XPS spectra of the AuNRs@ZIF−8@GO sample. A: full scan, B: Au 4f−Zn 3p scan, C: Zn 2p scan, D: C 1s scan.

Cyclic voltammetric behaviors of NA, DCP, CBZ, and DU

The voltammetric behaviors of NA, DCP, CBZ, and DU at bare GCE and AuNRs@ZIF−8@GO/GCE were examined by cyclic voltammetry (CV) (Fig. S2). At bare GCE (curve a), the oxidation potentials for NA, DCP, CBZ, and DU are about −0.14 V, 0.62 V, 0.74 V and 0.82 V. For NA, there is a symmetric cathodic peak on the reverse scan with the peak potential difference of 100 mV, indicating its quasi−reversible electrochemical oxidation process. However, the absence of cathodic peak on the reverse scan of DCP, CBZ, and DU molecules demonstrates that their oxidation reactions are irreversible processes. The electrochemical oxidation of NA, DCP, CBZ, and DU was then investigated by CV at the AuNRs@ZIF−8@GO/GCE (curve b). The AuNRs@ZIF−8@GO/GCE leads to somewhat negative shift in peak potentials, whereas it shows significant increase in peak currents when compared with the bare GCE. These results show that the modification of GCE with AuNRs@ZIF−8@GO results in an improvement in the overall electrochemical performance towards pesticides oxidation, which is due to the fact that this hierarchically sandwich−structured AuNRs@ZIF−8@GO accelerates the electrochemical reactions. In addition, the comparison of the background currents among the modified electrodes accords with the sequence of GCE < AuNRs@ZIF−8@GO/GCE, suggesting a gradually increased surface area of the electrode material and double layer capacitance.[4]

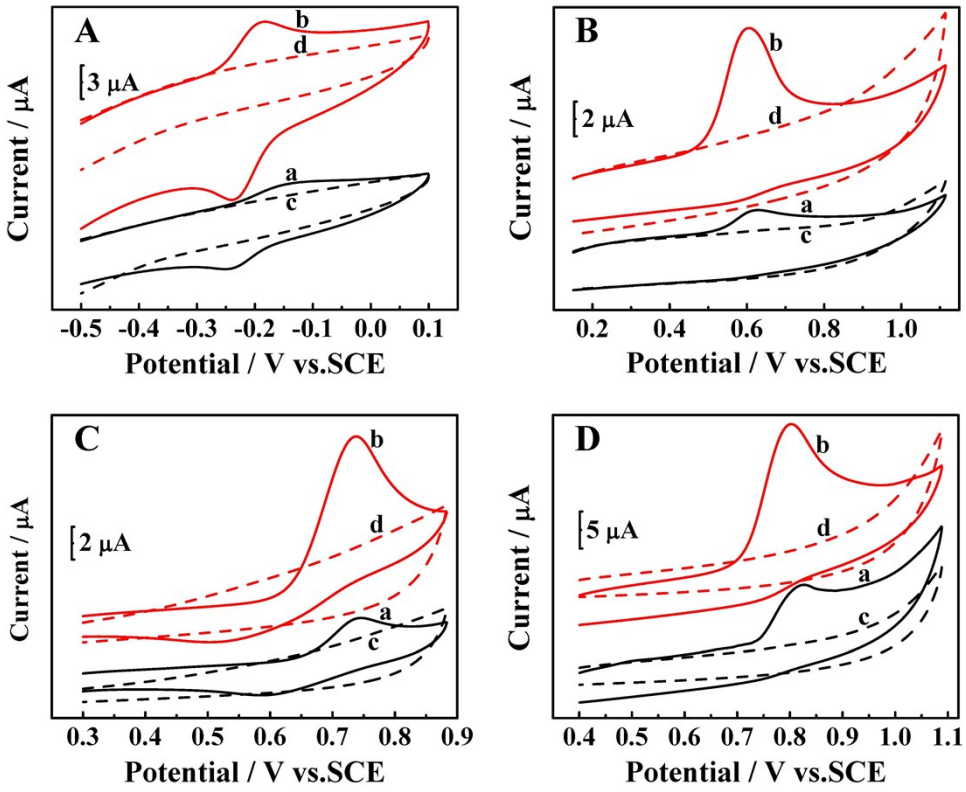

Fig. S2 Cyclic voltammograms of bare GCE (a,c) and AuNRs@ZIF−8@GO/GCE (b,d) in pH 7.96 B−R buffer with 50 μM NA (A), DCP (B), CBZ (C), and DU (D) and in blank. Scan rate: 150 mV s^{-1}.

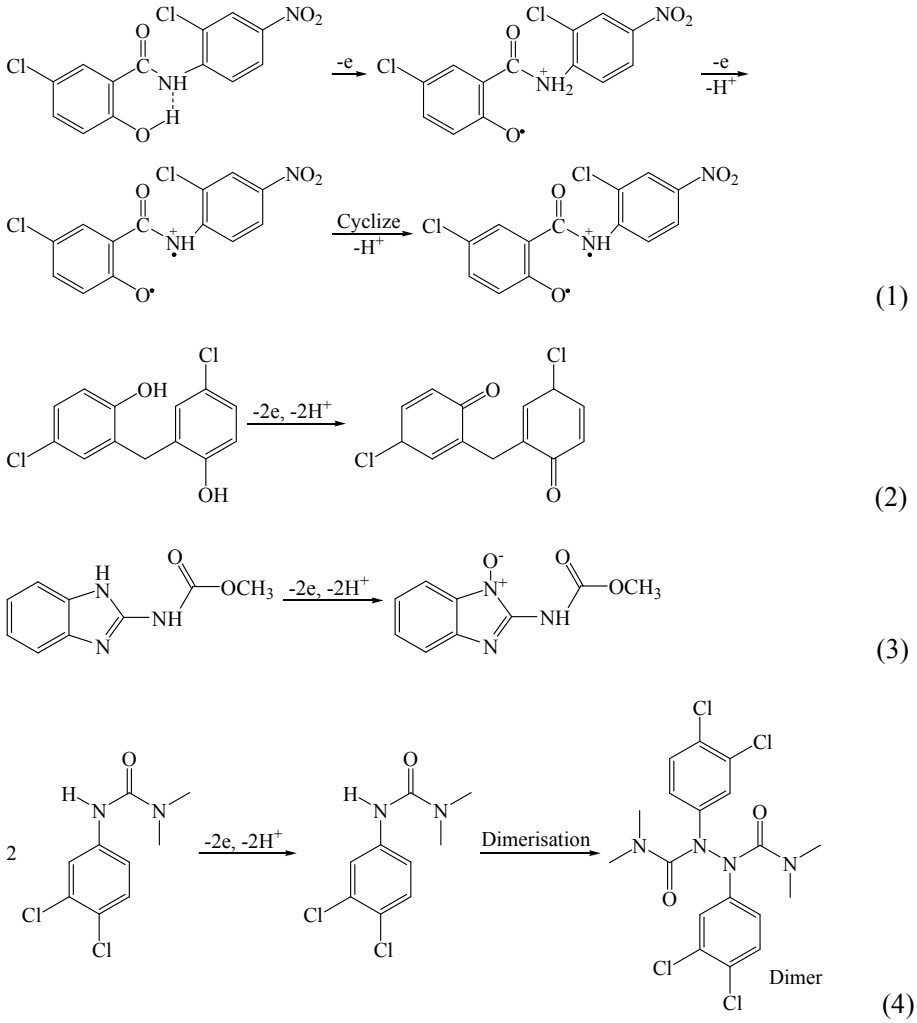

(1)

(2)

(3)

(4)

Fig. S3 The electrochemical reaction mechanisms of NA (1), DCP (2), CBZ (3), and DU (4).

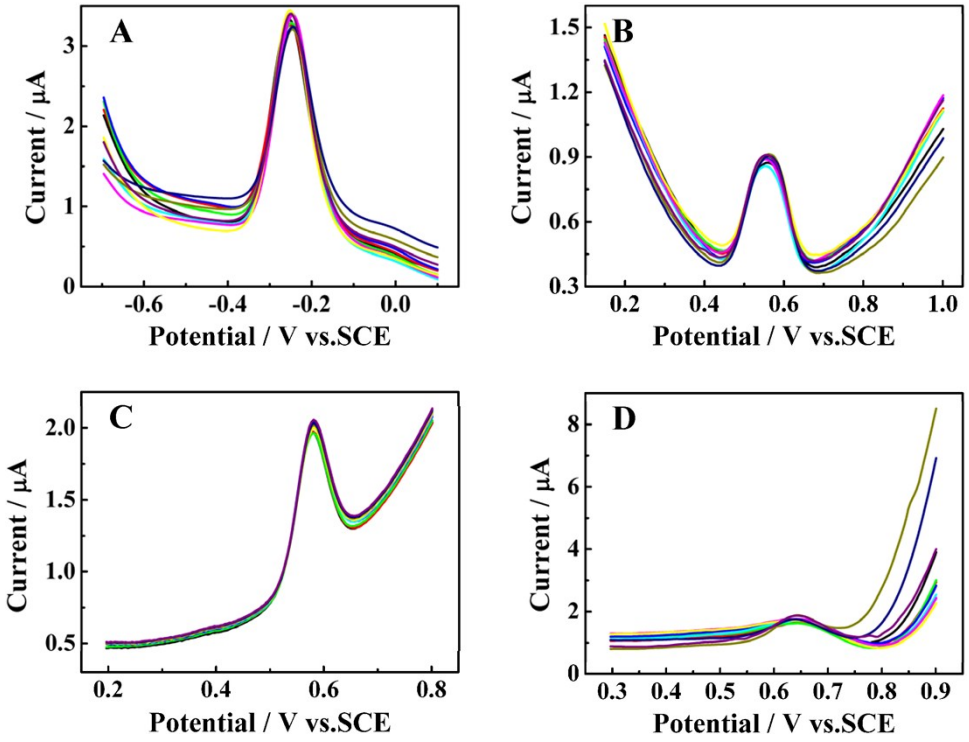

Fig. S4 Repeative differential pulse voltammetric detection of NA (A), DCP (B), CBZ (C), and DU (D) on ten AuNRs@ZIF−8@GO/GCEs.

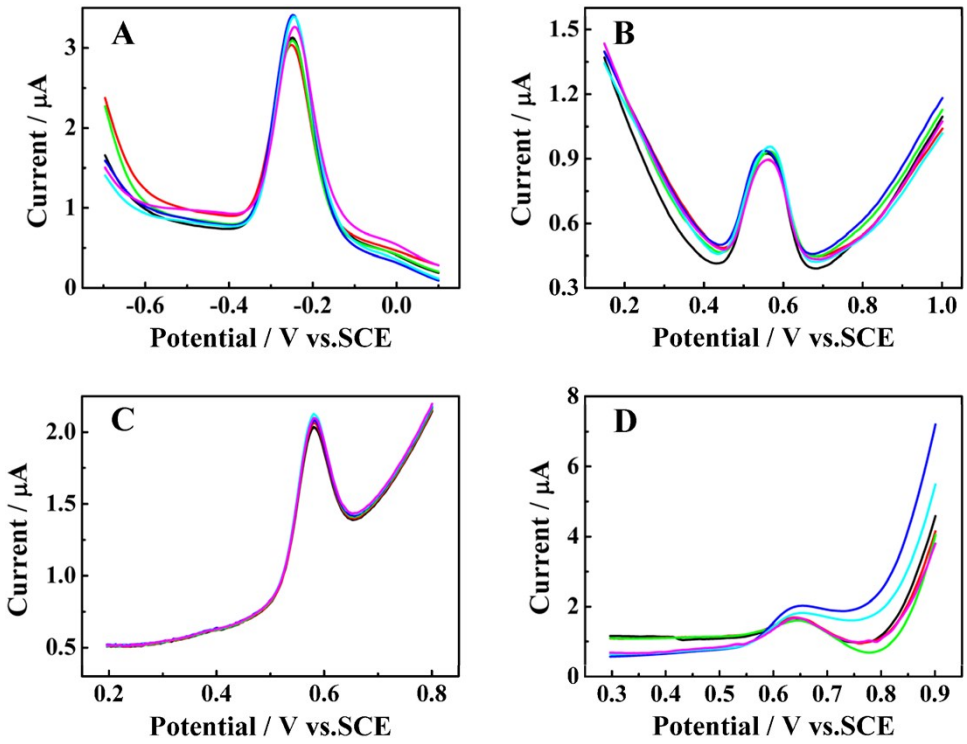

Fig. S5 Repeative differential pulse voltammetric detection of NA (A), DCP (B), CBZ (C), and DU (D) on the same AuNRs@ZIF−8@GO/GCE during thirty days.

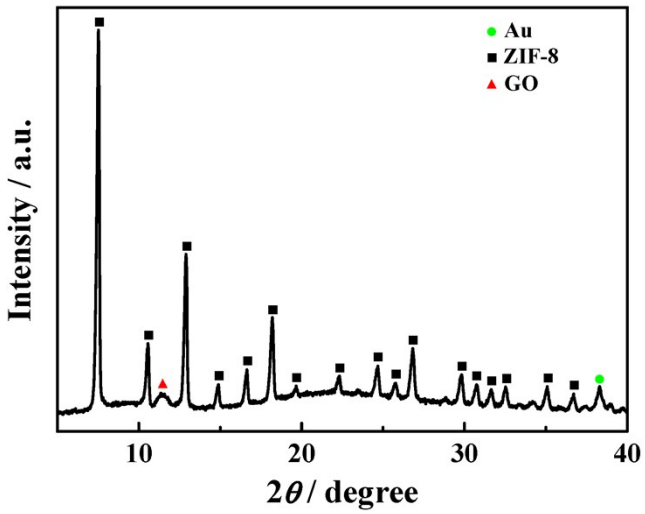

Fig. S6 PXRD pattern of Au@ZIF−8@GO after the stability test.

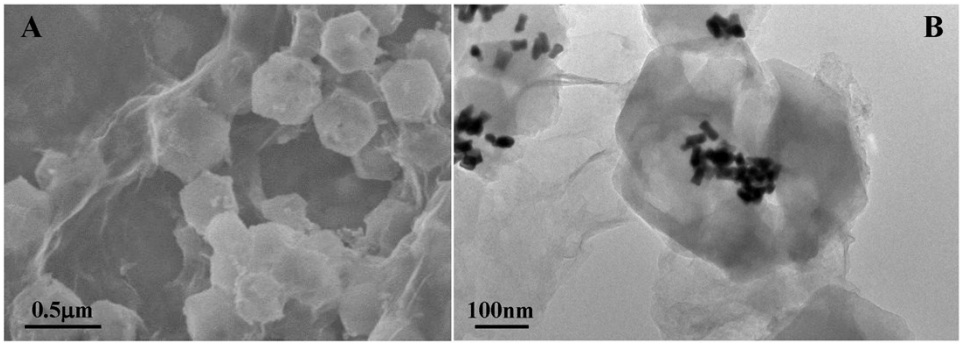

Fig. S7 SEM (A) and TEM (B) images of Au@ZIF−8@GO after the stability test.

Table S1 Performances comparison of different electrodes in literature for the electrochemical determination of NA, DCP, CBZ, and DU

Analytes	Working electrode	Linear range (μM)	LOD (nM)	Ref.
NA	Carbon nanoparticle−chitosan/GCE	0.01−2	7.7	5
	Poly(3,4−ethylenedioxythiophene)/GCE	0.075−7.50	10.9	6
	Pencil graphite electrode	0.05−10	15	7
	RGO[a]/GCE	0.020−23.1	6.6	8
	Pal−Gr−COOH[b]/GCE	0.02−0.99	4.6	9
	AuNRs@ZIF−8@GO/GCE	0.028−35	4.1	This work
DCP	β−CDs−MWCNTs[c]/GCE	0.05−2.9	14	10
	AuNRs@ZIF−8@GO/GCE	0.010−15	3.0	This work
CBZ	Cyclodextrin−graphene/GCE	0.005−0.45	2	11
	RGO/GCE	0.002−0.4	1.0	12
	PIL/OMCPE[d]	0.00654−4.18	2.62	13
	Zeolite/carbon paste electrode	0.0129−0.7777	1.5	14
	Graphene nanosheets/GCE	0.005−1.57	0.78	15
	AuNRs@ZIF−8@GO/GCE	0.0020−2.5	0.33	This work
DU	RGO−Au−Nafion/GCE	0.001−0.1	0.3	16
	SiO_2@Au/GCE	0.20−55	51.9	17
	Cathodically pretreated boron−doped diamond electrode	1.0−9.0	35	18
	AuNRs@ZIF−8@GO/GCE	0.0010−20	0.26	This work

[a] RGO: Reduced graphene oxide

[b] Pal−Gr−COOH: Palygorskite−carboxyl functionalized graphene

[c] β−CDs−MWCNTs: β−Cyclodextrins−multi−walled carbon nanotubes

[d] PIL/OMCPE: Pyrrolidinium ionic liquid modified ordered mesoporous carbon paste electrode

Notes and references

1 P. K. Chen, G. J. Lee, S. H. Davies, S. J. Masten, R. Amutha and J. J. Wu, *Mater. Res. Bull.*, 2013, **48**, 2375.

2 S. Luanwuthi, A. Krittayavathananon, P. Srimuk and M. Sawangphruk, *RSC Adv.*, 2015, **5**, 46617.

3 H. F. Wang, Y. S. Wang, A. Z. Jia, C. Y. Wang, L. M. Wu, Y. F. Yang and Y. J. Wang, *Catal. Sci. Technol.*, 2017, **7**, 5572.

4 Q. J. Wan, X. W. Wang, F. Yu, X. X. Wang and N. J. Yang, *J. Appl. Electrochem.*, 2009, **39**, 1145.

5 M. Ghalkhani and S. Shahrokhian, *Electrochem*. *Commun*., 2010, **12**, 66.

6 S. Mehretie, S. Admassie, M. Tessema and T. Solomon, *Sensor*. *Actuat*. *B−Chem*., 2012, **168**, 97.

7 E. Dede, Ö. Sağlam and Y. Dilgin, *Electorchim*. *Acta*, 2014, **127**, 20.

8 Y. Y. Yao, L. Zhang, X. M. Duan, J. K. Xu, W. Q. Zhou and Y. P. Wen, *Electrochim*. *Acta*, 2014, **127**, 86.

9 Z. X. Zhang, Y. Y. Yao, J. K. Xu, Y. P. Wen, J. Zhang and W. C. Ding, *Appl*. *Clay Sci*., 2017, **143**, 57.

10 K. Sipa, M. Brycht, A. Leniart, P. Urbaniak, A. Nosal−Wiercinska, B. Palecz and S. Skrzypek, *Talanta*, 2018, **176**, 625.

11 Y. J. Guo, S. J. Guo, J. Li, E. K. Wang and S. J. Dong, *Talanta*, 2011, **84**, 60.

12 X. Y. Dong, B. J. Qiu, X. W. Yang, D. Jiang and K. Wang, *Electrochemistry*, 2014, **82**,1061.

13 Y. Ya, T. S. Wang, L. P. Xie, J. J. Zhu, L. Tang, D. J. Xie and F. Y. Yan, *Anal*. *Methods*, 2015, **7**, 1493.

14 E. M. Maximiano, F. de Lima, C. A. L. Cardoso and G. T. Arrud, *J. Appl. Electrochem*., 2016, **46**, 713.

15 P. P. Wei, T. Gan and K. B. Wu, *Sensor. Actuat. B−Chem*., 2018, **274**, 551.

16 K. Zarei and A. Khodadadi, *Ecotox. Environ. Safe*., 2017, **144**, 171.

17 J. Y. Sun, T. Gan, R. Zhai, W. Q. Fu and M. M. Zhang, *Ionics*, 2018, **24**, 2465.

18 E. H. Duarte, J. Casarin, E. R. Sartori and C. R. T. Tarley, *Sensor. Actuat. B−Chem*., 2018, **255**, 166.